A Strains Activity of CuO Nanoparticles using Copper Chloride Dihydrate by Sol-Gel Method

B. Arunkumar[*], S. Johnson Jeyakumar and M. Jothibas

Department of Physics, T.B.M.L. College, Porayar-609307, India

*Corresponding author: E-mail: bvarun2030@gmail.com

Copper(II) oxide (CuO) nanoparticles synthesized by different molarities like 0.1, 0.2 and 0.3 M at calcinations temperature 450 ºC. The XRD results analyzed the prominent peaks corresponding to the monocrystalline nature of CuO nanoparticles and the average crystalline size of CuO nanoparticles size is decreased with increase of molarities. From SEM image of CuO nanoparticles, the particles are well scattered, which are well connected and consistent with the crystal system. The absorption spectra shows the blue shift which can be attributed to the small size of CuO nanostructures. The FTIR spectra confirmed high intense broad band peaks at 496.96 cm^{-1} and assigned to characteristics band of monoclinic phase CuO nanoparticles were synthesized and calcined at 450 ºC, and the particle size of the nanoparticles was found to be in the range of 19-23 nm. These sizes of integrated CuO nanoparticles is a cost-efficient, biological molecule capable of working with antibiotics against *Staphylococcus saprophyticus*, *Bacillus subtilis*, *Pseudomonas aeruginosa* and *Escherichia coli*.

Keywords: CuO nanoparticle, Antibacterial activity.

INTRODUCTION

In original sense of nanotechnology refers to the research ability to construct items from the bottom up, using techniques and tools being developed every day to make complete highly advanced product [1]. Nanotechnology as defined by the size naturally very broad, including fields of science as diverse as surface science, organic chemistry, molecular biology, semiconductor physics, microfabrication, *etc*. Nanotechnology may be able to create many new materials and devices with wide range of applications such as in medicine, electronics, biomaterials and energy production [2]. On the other hand, nanotechnology raises many of the same issues as any new technology. The design, characterization, production and application of structure, device and system by controlled manipulation of size and shape at the nanoscale have the superior characteristics and properties. This phenomenon has been creating crazy stimulation to researchers in the nanotechnology [3].

Research interests in microorganisms are highly appreciated for their phenomenal chemical and physiological aspects, but their differing variants, such as diffusivity, power resistance, electrostatic conductivity, strength and hardness, chemistry efficiency and various vital biological functions make the

difference and diversity [4]. These particles are widely used as medicinal catalysts, in clinical applications, in medical applications, in infections, antibiotics, fillers, catalysts, and semiconductors because they are very useful in the development of cosmetics and microelectronics [5].

The CuO is heavily convertible metal oxide by its attractive properties. It is used in various technology applications such as high temperature, tropical environments, gas sensors, and lighting applications [6]. Recently, it is used as an antimicrobial agent against various bacterial species. Copper(II) oxide crystal structures have a narrow gap, providing useful photocatalytic and photovoltaic properties [7]. Due to the various types of microorganisms, there is a problem in the microbial hybrid living conditions of air, water and soil and serious complications in health care. Due to spread of anti-antibiotic infections, the interest in alternative antimicrobial agents, such as small antibiotics, ketonic polymers, metal nanoparticles and antimicrobial peptides is increasing [8].

The synthesis method being an important parameter for control of particle size, morphology, crystallity and in order to achieve this goal CuO nanoparticles are investigated in different synthesis methods including precipitation such as sono chemical, sol-gel, hydrothermal, chemical path deposition

and spin coating sol-gel techniques [9,10]. Among these methods our preparation method for the synthesis of CuO nanoparticles belongs to sol-gel procedure .

The sol-gel process may be described as formation of an oxide network through polycondensation reactions of a molecular precursor in a liquid. A sol is a stable dispersion of colloidal particles or polymers in a solvent [11-13]. Compared to the ceramic method, dust was reduced and a sol-gel method was needed to have a low temperature. In addition, it should be possible to do the synthesis by remote control. Sol-gel method is a simple and relatively fast method. This method is often used by the level of nanoparticles to ensure strict control. This method allows for enormous control of the shape and shape of nanoparticles [14]. The idea behind sol-gel synthesis is to dissolve the compound in a liquid in order to bring it back as a solid in a controlled manner. Multicomponent compounds may be prepared with a controlled stoichiometry by mixing sols of different compounds. The sol-gel method prevents the problems with co-precipitation, which may be inhomogeneous [15], be a gelation reaction and it can enables mixing at an atomic level and results in small particles which are easily sinterable.

In this study, we have reported on the synthesis, characteristics and antimicrobial activity of CuO nanoparticles. CuO emphasizes the possibilities for acting as an antimicrobial agent of CuO nanoparticles and we coordinate different levels of CuO nanoparticles by controlling molarities during gel-combining research.

EXPERIMENTAL

The crystal structure and phase of CuO nanoparticles were characterized by X-ray diffraction (Shimadzu XRD 6000) analysis. The morphology of CuO nanoparticles was analyzed by scanning electron microscopy (Hitachi S-4450 SEM). The absorption spectra were measured using UV-Vis spectrophotometer (Shimadzu-UV 1800). Fourier transform infrared (FT-IR) spectra were recorded in the range 4000-450 cm^{-1} using a BRUKER: RFS 27.

Synthesis: The CuO nanoparticles were prepared by sol-gel method. Dissolved copper(II) chloride dihydrate (98 %, Merck, 0.1 M) in 100 mL deionized water. The prepared solution was heated at 80 ºC with constant stirring and 1 mL glacial acetic acid was added to the solution followed by the addition of 2M of NaOH dropwise. The colour of solution turned from blue to black immediately and resulted in the formation of black precipitate. The obtained black precipitate repeatedly washed 3 or 4 times with deionized water and filtered. Subsequently, the washed precipitate dried at 80 ºC for 24 h. Finally, the obtained powder was calcined at 450 ºC for 4 h. Similar, procedure has been followed to synthesize CuO nanoparticles using 0.2 and 0.3 M copper(II) chloride solution.

RESULTS AND DISCUSSION

Structural analysis: Fig. 1 shows the X-ray diffraction pattern for CuO nanoparticles prepared from different molarities. The two prominent peaks corresponding to the monocrystalline nature of CuO nanoparticles were observed. The high intensity peaks were observed at 35.4º, 38.6º and 48.6º, respective to the (111) (111), and (202) crystal planes matched with JCPDS
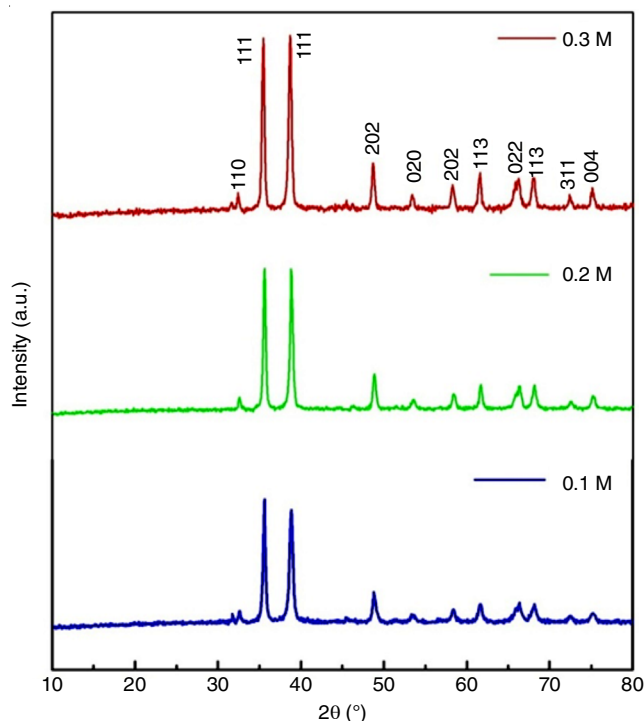
Fig. 1. XRD diffraction pattern of CuO nanoparticles at different molarities

card No. 801916. No other peaks have been found within the detection range of the XRD pattern [16].

All the diffraction peaks are coded as the usual monoclinic structure. The average crystalline size of CuO nanoparticles is calculated using the Scherrer's formula, which detected nanopareticles size as 19-23 nm. The results confirm that spread of multiple peaks which indicates that crystal is small [17].

The calculated replication of XRD results has a greater value for 20 nm smaller particles and shows that the particle size is high. It is clear that smaller particles have greater strain and larger particles have less strain. The structural parameters are calculated from the full-width half maximum and suggest that the decrease in particle size, stacking fault, micro-strain and dislocation index is also decreases [18]. On comparing with the standard samples (JCPDS card No. 801916), the X-ray diffractogram and 2θ values of CuO were found to be in fairly good agreement, thus containing the monoclinic crystal structure. The broadening in the diffraction peaks might be due to the size effect and the crystallite size is in the nano-regime.

These nanocrystal have lesser lattice planes compared to the bulk, which calculate to the broadening of the peaks in the diffraction pattern. It could also arise due to lack of sufficient energy needed by atoms to move to a proper site in forming the crystallite. The width of peaks becomes large as the particle become smaller and also width of peaks becomes small as the particles become larger [19,20]. The crystallite size has been inferred from 2θ and the full width at half maximum (FWHM) of the (111) Diffraction peak on the basis of Scherrer's relation,

$$D = \frac{K\lambda}{\beta\cos\theta} \qquad (1)$$

where D is the average crystallite size in Å, K is the shape factor (0.9), λ is the wavelength of X-ray, θ is the Bragg angle and β is the corrected line broadening of the nanoparticles.

The result shows that the average crystallite size of nano-CuO is about 19-23 nm. The estimated values of crystallite sizes and structural parameters including dislocation density (δ), micro-strain (ε) and stacking fault (SF) of monoclinic CuO nanoparticles are summarized in Table-1.

The microstrain (ε) is calculated using the relation:

$$\varepsilon = \frac{\beta\cos\theta}{4} \qquad (2)$$

$$\text{Dislocation density } (\delta) = \frac{1}{D^2} \qquad (3)$$

$$\text{Stacking Fault}\left(SF = \frac{2\pi^2}{45(3\tan\theta)^{1/2}}\right)\beta \qquad (4)$$

The values in Table-1 confirmed that as crystal size decreases while stacking fault, micro strain and dislocation density are increased. In this work, it is concluded in copper oxide nanoparticles, the basic crystal of integrated pile, such as CuO has become apparent, but the queue peaks are strong after calcination process because of thermal treatment gives sufficient nuclear energy to form CuO crystalline [21,22]. These strong peaks of CuO formation can be obtained from a sol-gel method as confirmed in XRD analysis and also the excellent crystalline of CuO is derived from $CuCl_2$ precedents the effect of crystallization and its size can be achieved efficiently.

Additionally from the XRD spectra, it is inferred that the variation is observed between full width half maxima (FWHM) and crystal size. It was also observed that with increase in different molarities, broadening of the peaks increased and while the full width at half maxima (FWHM) increased and crystal size is equally decreased as shown in Fig. 2. The FWHM value for crystals obtained at 0.3 M was 0.4521, which is significantly very low compared to crystals obtained at 0.1M (0.37). Extending the high FWHM value and increased peak, the combined CuO powder has become much higher crystalline with the reduction of different molarities (Fig. 2). From the structural analyses, the fitted patterns are in agreement with the respective experimental data confirming the formation of single pure CuO phase without the presence of any additional phases or impurities.

Morphological analysis: From the SEM images (Fig. 3) of CuO nanoparticles, it is learnt that the particles are well scattered, well-connected and consistent with the crystal structure. There was also a high intensity character. Fig. 3 also shows for the formation of well-nanotablet tube model and regular shaped CuO nanoparticle. Due to high surface charge, agglomeration and aggregation crystals are clearly visible and integrated. The representation of the grains is regular and the microstructure consists of many neatly arranged rod shaped particles (nano-tablet tube).
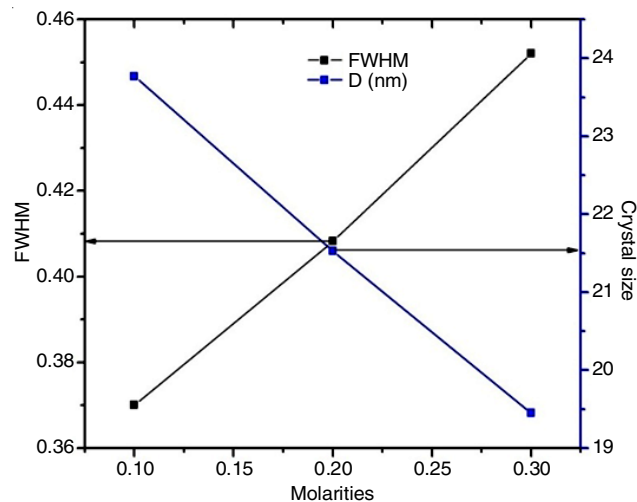
Fig. 2.   Variation of FWHM and crystal size of CuO nanoparticles at different molarities
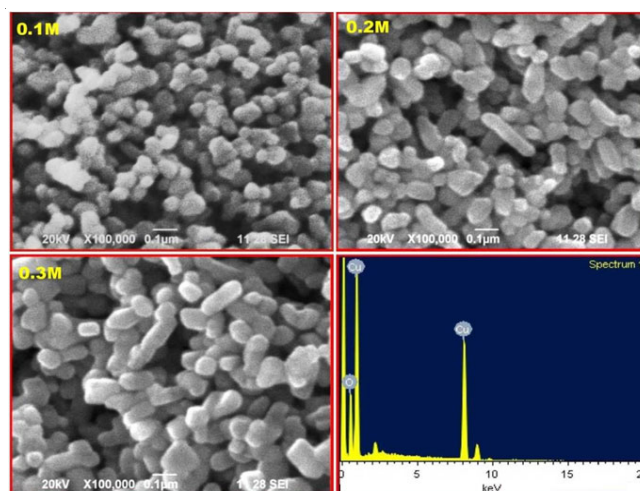
Fig. 3. Morphological analysis of CuO nanoparticles at different molarities

The molecular mechanism of the solvent polarity is thought to affect the properties of nanoparticles [23]. The main features of these particles are almost rod and their diameter is distributed simultaneously. The given copper oxide nanoparticles have a relatively small tube particle that has the same size. The size of CuO nanoparticles decreases (Table-1) with increase in molar concentrations up to 0.3 M of $CuCl_2\cdot2H_2O$ but increases, thereafter which is consistent with the information obtained from XRD calculations. When the concentration was increased from 0.1 to 0.3 M, small particles appear and the relatively large particles became dominant. This shows that the higher concentration results in particle growth in consistent with the literature [24,25]. The SEM results also confirmed the decrease in the particle size with increase in concentration of molarities which agreed well with the XRD results [26].

TABLE-1 STRUCTURAL PARAMETER OF CuO NANOPARTICLES FORMED AT DIFFERENT MOLARITIES						
Molarities (M)	FWHM	2θ	Crystal size (nm)	Stacking Fault	Dislocation density $\delta \times 10^{14}$	Micro strain (ε)
0.1	0.3700	38.7961	23.77	0.002752	1.77056	0.001523
0.2	0.4082	38.6394	21.53	0.003043	2.15710	0.001681
0.3	0.4521	38.7971	19.45	0.003362	2.64347	0.001861

UV-visible analysis: Fig. 4 shows the absorption spectra of CuO nanoparticles prepared at different molarities. The absorption edge values are found to be 360-378 nm for 0.1-0.3 M. The optical band gap energy has been calculated using the following equation:

$$(\alpha h\nu) = A(h\nu - E_g)^n \qquad (5)$$

where A is a constant, E_g is the band gap of material, ν is the frequency of incident radiation, h is the Planck's constant and the exponent n is 2 for allowed direct band transitions. The calculated energy band gap values (3.36-3.40 eV) are higher than that of the value for bulk CuO (1.2 eV) indicates the blue shift. Higher direct band gap as compared to bulk value indicating blue shift of band gap due to the quantum confinement effect [27,28]. This blue shift can be attributed to the small size of CuO nanostructures. The observed results are in good agreement with the previous reports of CuO [29,30].
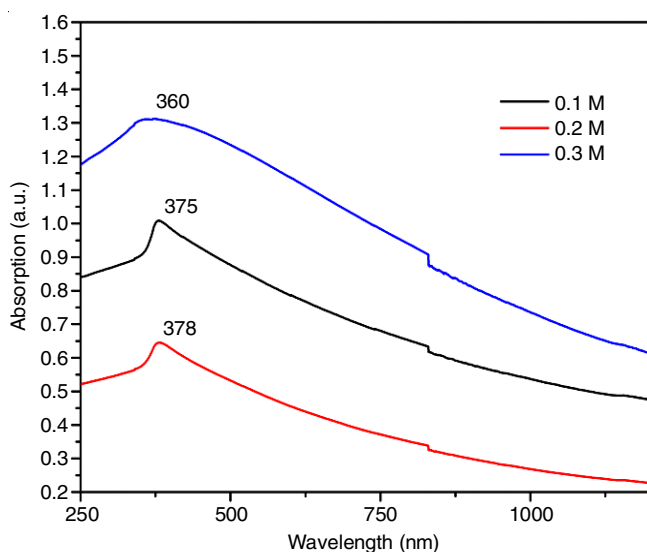
Fig. 4. UV absorbance of CuO nanoparticles at different molarities

FTIR analysis: Fig. 5 shows the FTIR spectra of CuO nanoparticles synthesized at different molar concentrations. From these spectra, the various compositional elements and their bonding nature present in the CuO nanoparticles were analyzed. The low intense broad band peaks at 496.96 cm⁻¹ are assigned to characteristics band of monoclinic phase CuO nanoparticles. The peaks at 1383 and 1626 cm⁻¹ are due to carbonyl C=O stretching bonds [31]. Moreover, the broad peaks at 3419 cm⁻¹ are ascribed to the stretching and bending vibration mode of O-H bond. Finally, a tiny tip at 2364 cm⁻¹ is due to the absorption of atmospheric CO_2 [32,33].

Antibactrial activity: The effectiveness of bacteria against microorganisms that have been studied by CuO nanoparticles. This will be carried out on both Gram positive and Gram negative organisms like *Staphylococcus saprophyticus*, *Bacillus subtilis*, *Pseudomonas aeruginosa* and *Escherichia coli* using sterile media like Mueller-Hinton agar by disc diffusion method. The results are showed in Table-2. The potential technique associated with the function of bacteria may be caused by cell membrane [34,35]. The released of copper ions from CuO nanoparticles, which negatively attached the bacterial cell wall to the charging and fracture, causing protein attenuation and cell death [36-38].
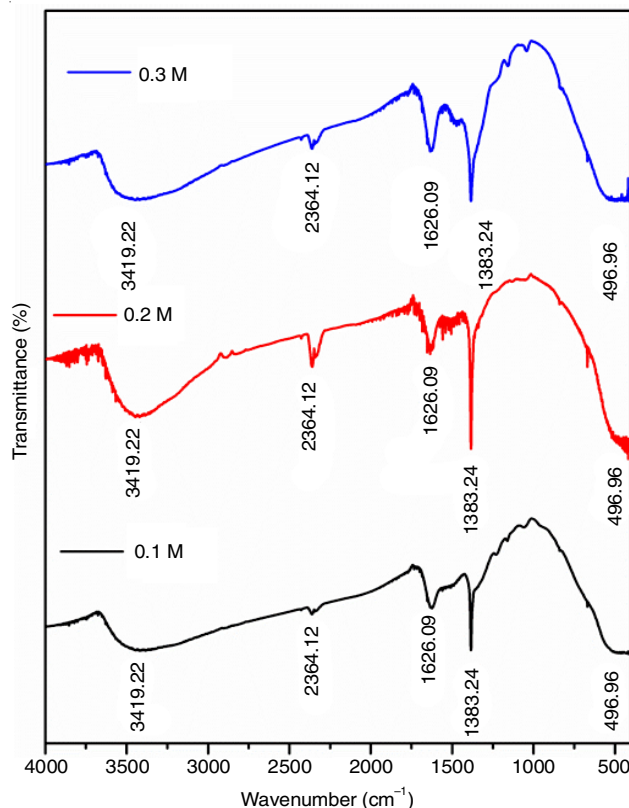
Fig. 5. FTIR spectra of CuO nanoparticles at different molarities

TABLE-2
ANTIBACTERIAL ACTIVITY OF CuO NANOPARTICLES AT DIFFERENT MOLARITIES

Bacteria	Standard antibiotic disc	Zone of inhibition (mm)		
		0.1 M	0.2 M	0.3 M
B. subtilis	18	12	16	09
E. coli	20	10	19	10
P. aeruginosa	21	05	11	08
S. pyogenes	19	11	12	10

In addition, the bacterial cells interfere with the important biochemical functions of copper ion processes [39,40].

Conclusion

The CuO nanoparticles have been synthesized by a simple effective sol-gel method. The formation of high purity monoclinic phase of CuO nanoparticles was confirmed from XRD analysis. From XRD results, it is also revealed that the crystal size decrease with increase of molar concentration. The SEM micrograph confirms the formation of nano-tablet tube shape CuO nanoparticles with negligible agglomeration. The optical band gap of CuO nanoparticles were found to increase with increase of molar concentration which is due to size quantization effect. The sol-gel system of integrated CuO nanoparticles is a cost-efficient, biological molecule capable of working with antibiotics against Gram positive and Gram negative bacteria like *Staphylococcus saprophyticus, Bacillus subtilis, Pseudomonas aeruginosa* and *Escherichia coli*.

CONFLICT OF INTEREST

The authors declare that there is no conflict of interests regarding the publication of this article.

REFERENCES

1. S. Eustis and M.A. El-Sayed, *Chem. Soc. Rev.*, **35**, 209 (2006); https://doi.org/10.1039/B514191E.
2. M. Rakesh, T.N. Divya, T. Vishal and K. Shalini, *J. Nanomed. Biotherap. Discov.*, **5**, 131 (2015); https://doi.org/10.4172/2155-983X.1000131.
3. A.C.S. Samia, S. Dayal and C. Burda, *J. Photochem. Photobiol. Chem.*, **82**, 617 (2006); https://doi.org/10.1562/2005-05-11-IR-525.
4. K.S. Kim, W.H. Baek, J.M. Kim, T.S. Yoon, H.H. Lee, C.J. Kang and Y.S. Kim, *Sensors*, **10**, 765 (2010); https://doi.org/10.3390/s100100765.
5. J. Singh, G. Kaur and M. Rawat, *J. Bioelectron. Nanotechnol.*, **1**, 5 (2016).
6. F. Martinez-Gutierrez, P.L. Olive, A. Banuelos, E. Orrantia, N. Nino, E.M. Sanchez, F. Ruiz, H. Bach and Y. Av-Gay, *J. Nanomed.*, **6**, 681 (2010); https://doi.org/10.1016/j.nano.2010.02.001.
7. M.J. Guajardo-Pacheco, J.E. Morales-Sánchez, J. González-Hernández and F. Ruiz, *Mater. Lett.*, **64**, 1361 (2010); https://doi.org/10.1016/j.matlet.2010.03.029.
8. A. Kumar, K. Perumal and P. Thirunavukkarasu, *J. Optoelectron. Adv. Mater. Rapid Commun.*, **4**, 831 (2010).
9. L.G. Carrascosa, M. Moreno, M. Alvarez and L.M. Lechuga, *TrAC Trends Anal. Chem.*, **25**, 196 (2006); https://doi.org/10.1016/j.trac.2005.09.006.
10. S. Amrut, J. Satish, B. Ramchandara and S. Raghumani, *J. Adv. Appl. Sci. Res.*, **1**, 36 (2010).
11. K.R. Chandrika, P. Kiranmayi and R.V.S.S.N. Ravikumar, *Asian J. Pharm. Clin. Res.*, **5**, 97 (2012).
12. L. Qi, Z. Xu, X. Jiang, C. Hu and X. Zou, *Carbohydr. Res.*, **339**, 2693 (2004); https://doi.org/10.1016/j.carres.2004.09.007.
13. J.P. Ruparelia, A.K. Chatterjee, S.P. Duttagupta and S. Mukherji, *Acta Biomater.*, **4**, 707 (2008); https://doi.org/10.1016/j.actbio.2007.11.006.
14. R. Vijayalakshmi and V. Rajendran, *Arch. Appl. Sci. Res.*, **4**, 1183(2012).
15. R. Dobrucka and J. Dlugaszewska, *Saudi J. Biol. Sci.*, **23**, 517 (2016); https://doi.org/10.1016/j.sjbs.2015.05.016.
16. K. Nithya, P. Yuvasree, N. Neelakandeswari, N. Rajasekaran, K. Uthayarani, M. Chitra and S.S. Kumar, *Int. J. ChemTech Res.*, **6**, 2220 (2014).
17. J. Morales, L. Sánchez, F. Martín, J.R. Ramos-Barrado and M. Sánchez, *Electrochim. Acta*, **49**, 4589 (2004); https://doi.org/10.1016/j.electacta.2004.05.012.
18. N.P.S. Acharyulu and R.S. Dubey, *Int. J. Eng. Res. Technol.*, **3**, 639 (2014).
19. Y. Aparna, K.V. Enkateswara Rao and P.S. Subbarao, *Int. Proc. Chem. Biol. Environ. Eng.*, **48**, 156 (2012).
20. M. Jothibas, S.J. Jeyakumar, C. Manoharan, I.K. Punithavathy, P. Praveen and J.P. Richard, *J. Mater. Sci.: Mater. Electron.*, **28**, 1889 (2017); https://doi.org/10.1007/s10854-016-5740-6.
21. R.S. Kumar, S.J. Jeyakumar, M. Jothibas, I.K. Punithavathy and J.P. Richard, *J. Mater. Sci.: Mater. Electron.*, **28**, 20 (2017); https://doi.org/10.1007/s10854-017-7456-7.
22. K. Phiwdang, S. Suphankij, W. Mekprasart and W. Pecharapa, *Energy Procedia*, **34**, 740 (2012); https://doi.org/10.1016/j.egypro.2013.06.808.
23. M. Arakha, J. Roy, P.S. Nayak, B. Mallick and S. Jha, *Free Radic. Biol. Med.*, **110**, 42 (2017); https://doi.org/10.1016/j.freeradbiomed.2017.05.015.
24. W. Wang, L. Wang, H. Shi and Y. Liang, *CrystEngComm*, **14**, 5914 (2012); https://doi.org/10.1039/c2ce25666e.
25. S.M. Sathiya, G.S. Okram and M.A. Jothi Rajan, *Adv. Mater. Process.*, **2**, 371 (2017); https://doi.org/10.5185/amp.2017/605.
26. S. Ravi, A.B. Kaiser and C.W. Bumby, *J. Appl. Phys.*, **118**, 085311 (2015); https://doi.org/10.1063/1.4929644.
27. J. Shi, J. Wang, W. Yang, Z. Zhu and Y. Wu, *Mater. Res.*, **19**, 316 (2016); https://doi.org/10.1590/1980-5373-MR-2015-0491.
28. A.I. El-Batal, H.H. El-Hendawy and A.H.I. Faraag, *BioTechnologia*, **98**, 225 (2017); https://doi.org/10.5114/bta.2017.70801.
29. P. Tippayawat, N. Phromviyo, P. Boueroy and A. Chompoosor, *PeerJ*, **4**, e2589 (2016); https://doi.org/10.7717/peerj.2589.
30. P. Mallick and S. Sahu, *Nanosci. Nanotechnol.*, **2**, 71 (2012); https://doi.org/10.5923/j.nn.20120203.05.
31. F. Ijaz, S. Shahid, S.A. Khan, W. Ahmad and S. Zaman, *Trop. J. Pharm. Res.*, **16**, 743 (2017); https://doi.org/10.4314/tjpr.v16i4.2.
32. J.K. Sharma, P. Srivastava, G. Singh, M.S. Akhtar and S. Ameen, *Thermochim. Acta*, **614**, 110 (2015); https://doi.org/10.1016/j.tca.2015.06.023.
33. S. Sumitha, R.P.Vidhya, M.S. Lakshmi and K.S. Prasad, *Int. J. Chem. Sci.*, **14**, 435 (2016).
34. S. Ahmed, M. Ahmad, B.L. Swami and S. Ikram, *J. Adv. Res.*, **7**, 17 (2016); https://doi.org/10.1016/j.jare.2015.02.007.
35. A. Haider, S. Kwak, K.C. Gupta and I.-K. Kang, *J. Nanomater.*, **2015**, Article ID 832762 (2015); https://doi.org/10.1155/2015/832762.
36. P.P.N.V. Kumar, U. Shameem, P. Kollu, R.L. Kalyani and S.V.N. Pammi, *Bionanoscience*, **5**, 135 (2015); https://doi.org/10.1007/s12668-015-0171-z.
37. V. Vellora, T.Padil and M. Èerník, *Int. J. Nanomed.*, **8**, 889 (2013); https://doi.org/10.2147/IJN.S40599.
38. P. Ghorbani, M. Soltani, M. Homayouni-Tabrizi, F. Namvar, S. Azizi, R. Mohammad and A. Moghaddam, *Molecules*, **20**, 12946 (2015); https://doi.org/10.3390/molecules200712946.
39. C. Tang, W. Sun and W. Yan, *RSC Adv.*, **4**, 523 (2014); https://doi.org/10.1039/C3RA44799E.
40. H.M.M. Ibrahim, *J. Radiation Res. Appl. Sci.*, **8**, 265 (2015). https://doi.org/10.1016/j.jrras.2015.01.007.